X-ray Luminosity Function and Clustering of AGNs: Implications for AGN Evolution

(Sorry for the title change)

Takamitsu Miyaji

Instituto de Astronomía sede Ensenada
Universidad Nacional Autónoma de México
Campus Ensenada

Scope

- X-ray Luminosity Function and Evolution
  - Latest results including COSMOS survey
  - Comparison with semi-analytical models/simulations.
    - Indication of two modes of AGN evolution?
- Clues from the AGN clustering and Halo Occupation Distribution
  - Clustering and Host Halo mass of AGNs in various classes
  - Halo Occupation Distribution

Detailed Shape of Evolutionary Behavior of the X-ray Luminosity Function (XLF) of Active Galactic Nuclei

(XLF for Compton-thin AGNs)

Miyaji, Hasinger, COSMOS Team (2015)

AGN X-ray Spectra

Rest frame X-ray spectra

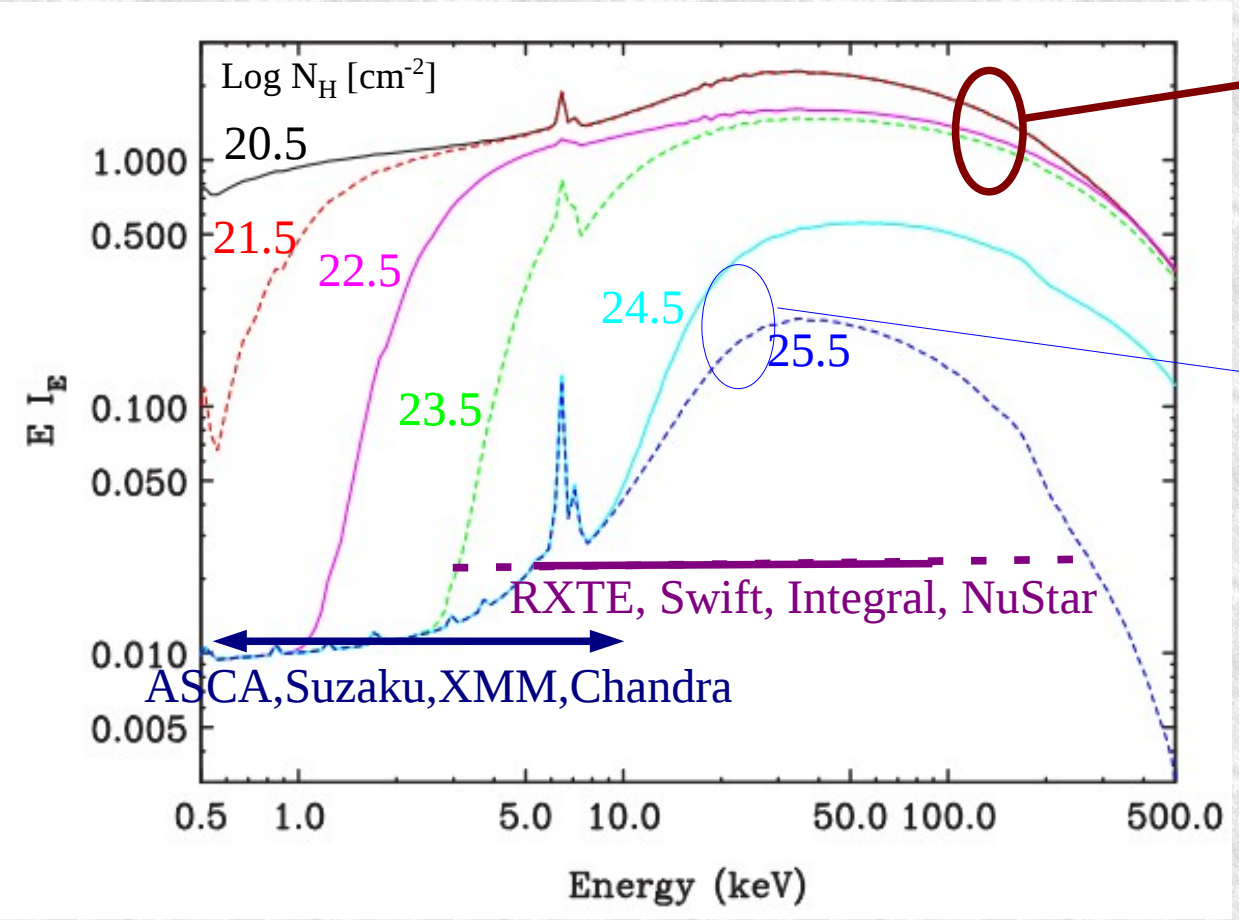

Ueda, Akiyama, Hasinger, TM et al. 2014

Compton-thin AGN

E<~10 keV: Photoelectric absorption at $N_H<10^{24}$ cm^{-2}

E>~10 keV: unabsorbed.

Compton-thick AGN

X-ray photons going through an $N_H \sim \sigma_T^{-1} > \sim 10^{24} cm^{-2}$ column of gas is subject to Compton scattering:

E<10 keV: Deep Photoelectric absorption

E>10 keV: Compton scattering at log N_H~>24. Extended path/loss of energy and subsequent photoelectric absorption.

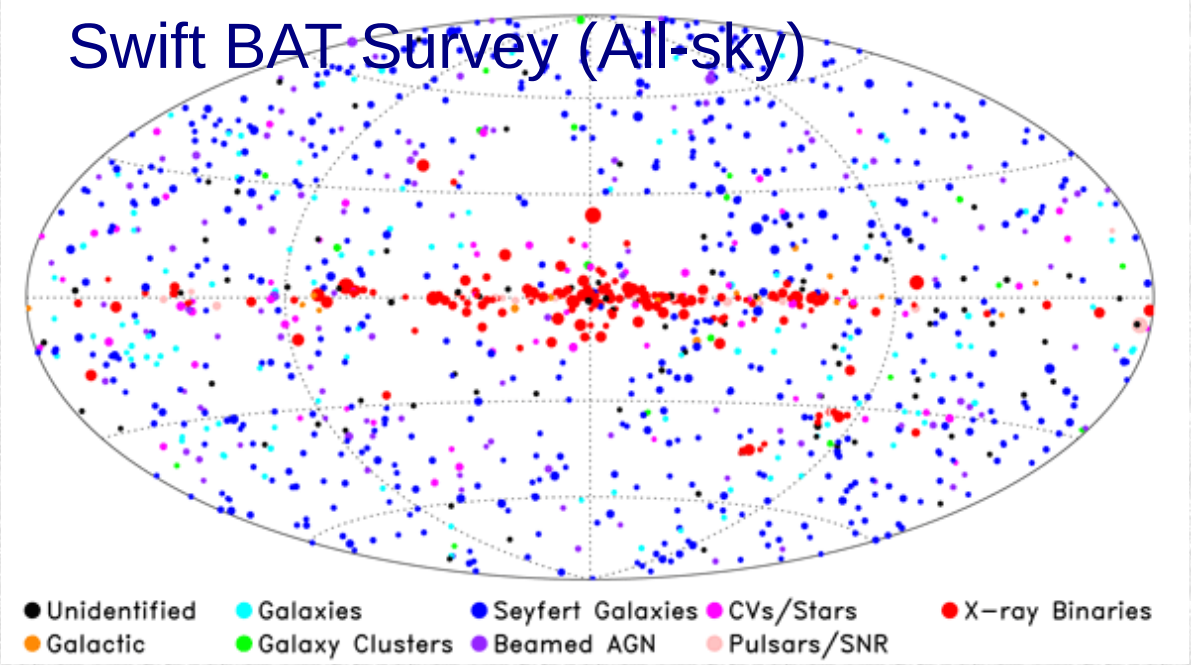

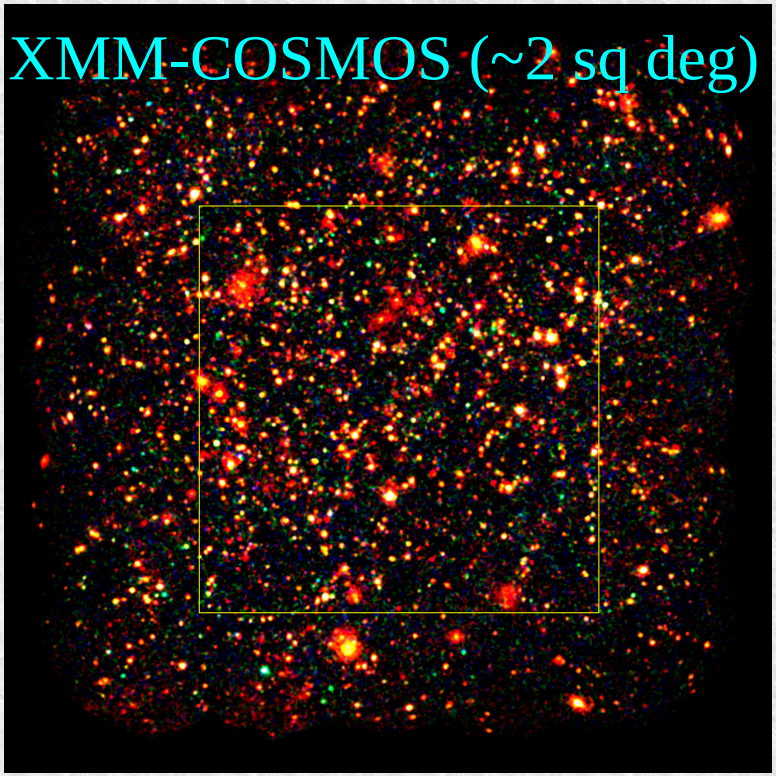

Collecting Results of the Surveys in full range of depth/area

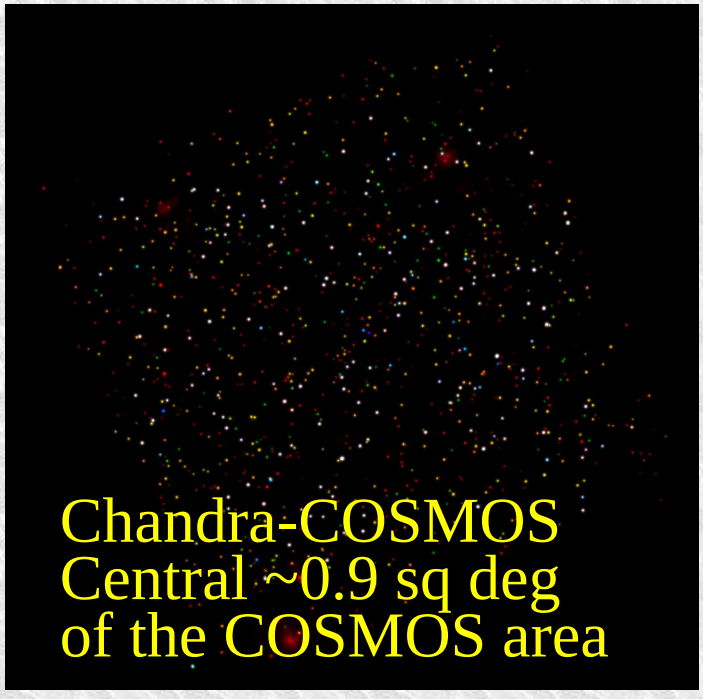

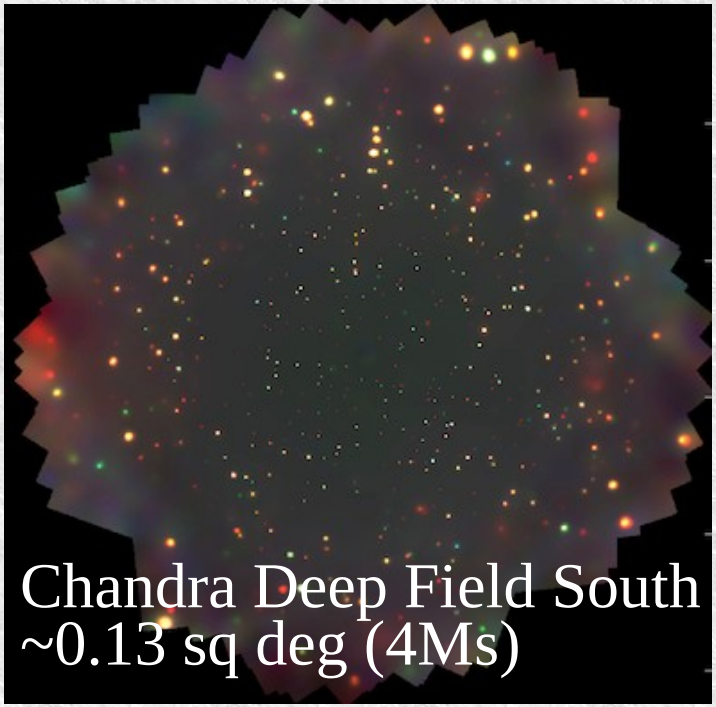

Hard X-ray Surveys (mainly 2-10 keV)

Combination of various surveys
from all-sky (Swift BAT) to the deepest (Chandra Deep Field South)

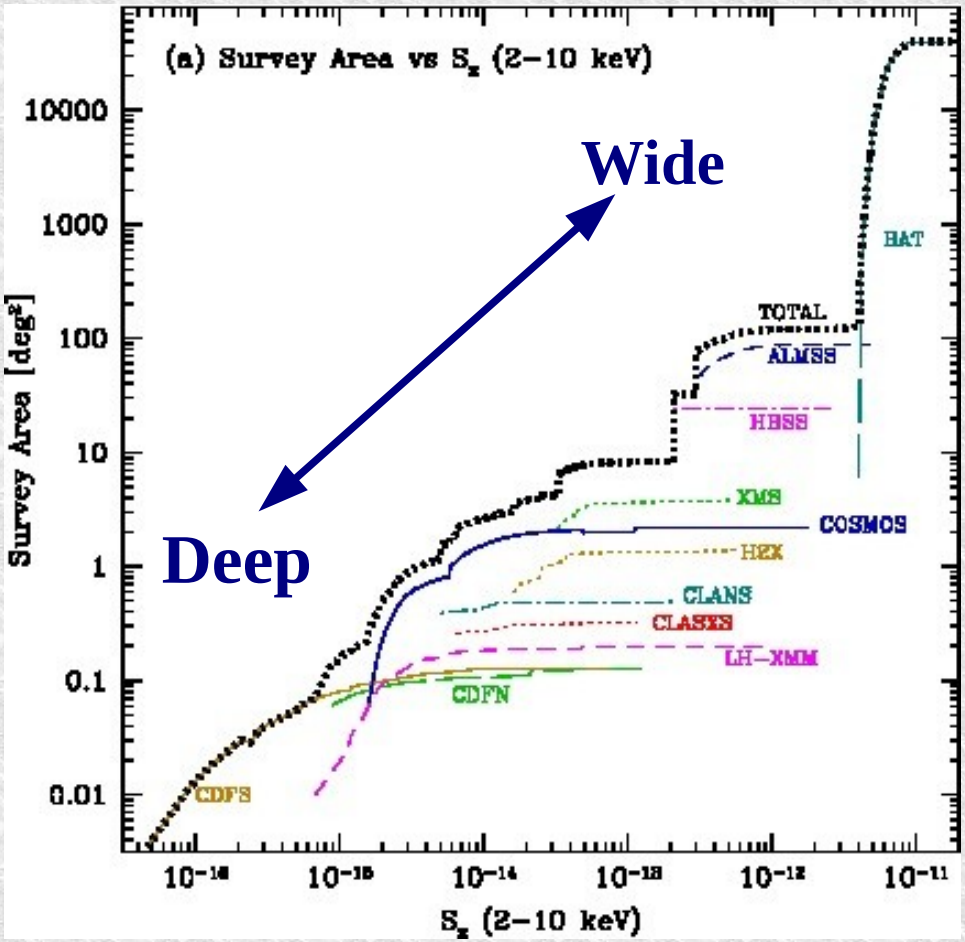

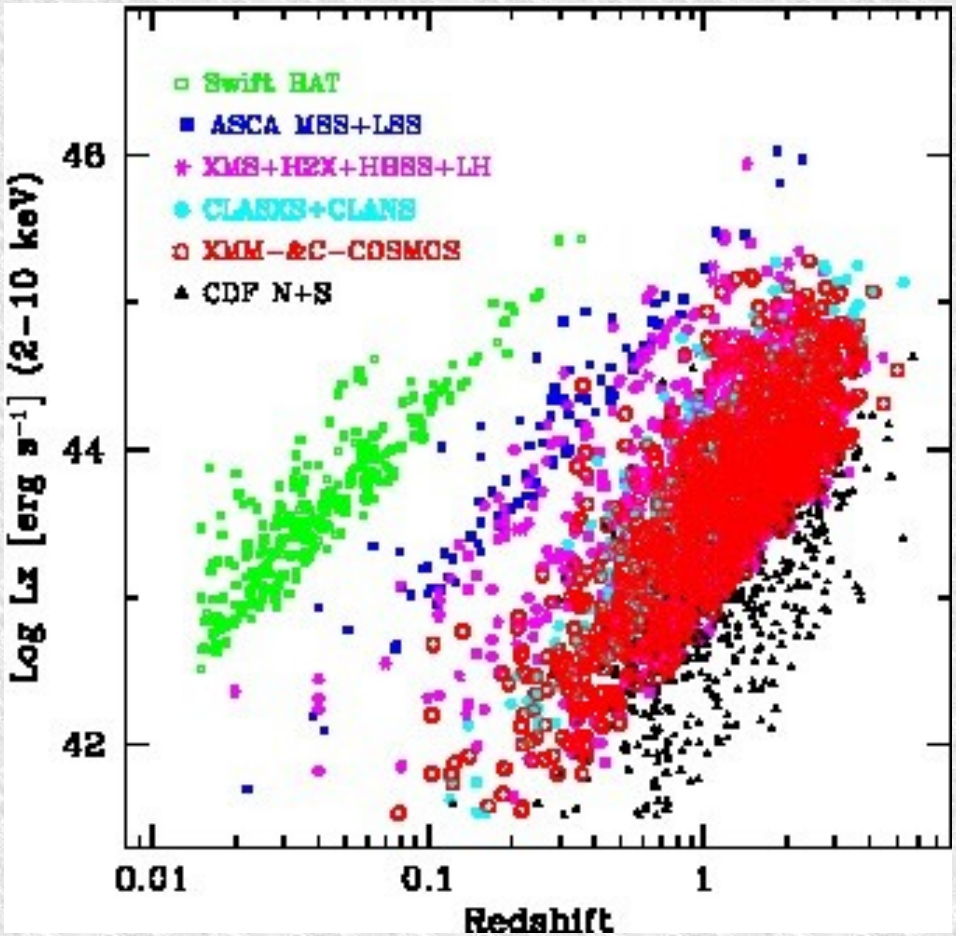

~3200 AGNs, ~40% of which are from the COSMOS survey

Miyaji, Hasinger, COSMOS Team (2015)

Analysis Aspects - I

- Luminosity defined as the 2-10 keV intrinsic luminosity
- Correction for absorption using template spectra and NH function of Ueda et al. (2014).
- Swift BAT 15-55 keV (Ajello+'12) coverted to 2-10 keV using unabsorbed AGN template.
- Removal of a small number of known Compton-thick AGNs from sample.
- Fit to analytical functions using the Maximum-likelihood technique.
  - Global expression using the Luminosity-dependent Density Evolution model.
  - Fit each redshift shell to smoothed two power-law form.
  - Fit each luminosity class to 3-segment $(1+z)^p$ form.

Analysis Aspects-II

- Binned XLF with N_{obs}/N_{mdl} method.
  - N_{obs}: Obserbed number
  - N_{mdl}: Model expected number.
  - Scale model value by (N_{obs}/N_{mdl})
- Not all objects have accurate spectroscopic redshifts. For some objects, rely on photometric redshifts.
  - Include the probability distribution function (PDF) of the photometric redshifts into the fitting process, whenever available (COSMOS+LH).

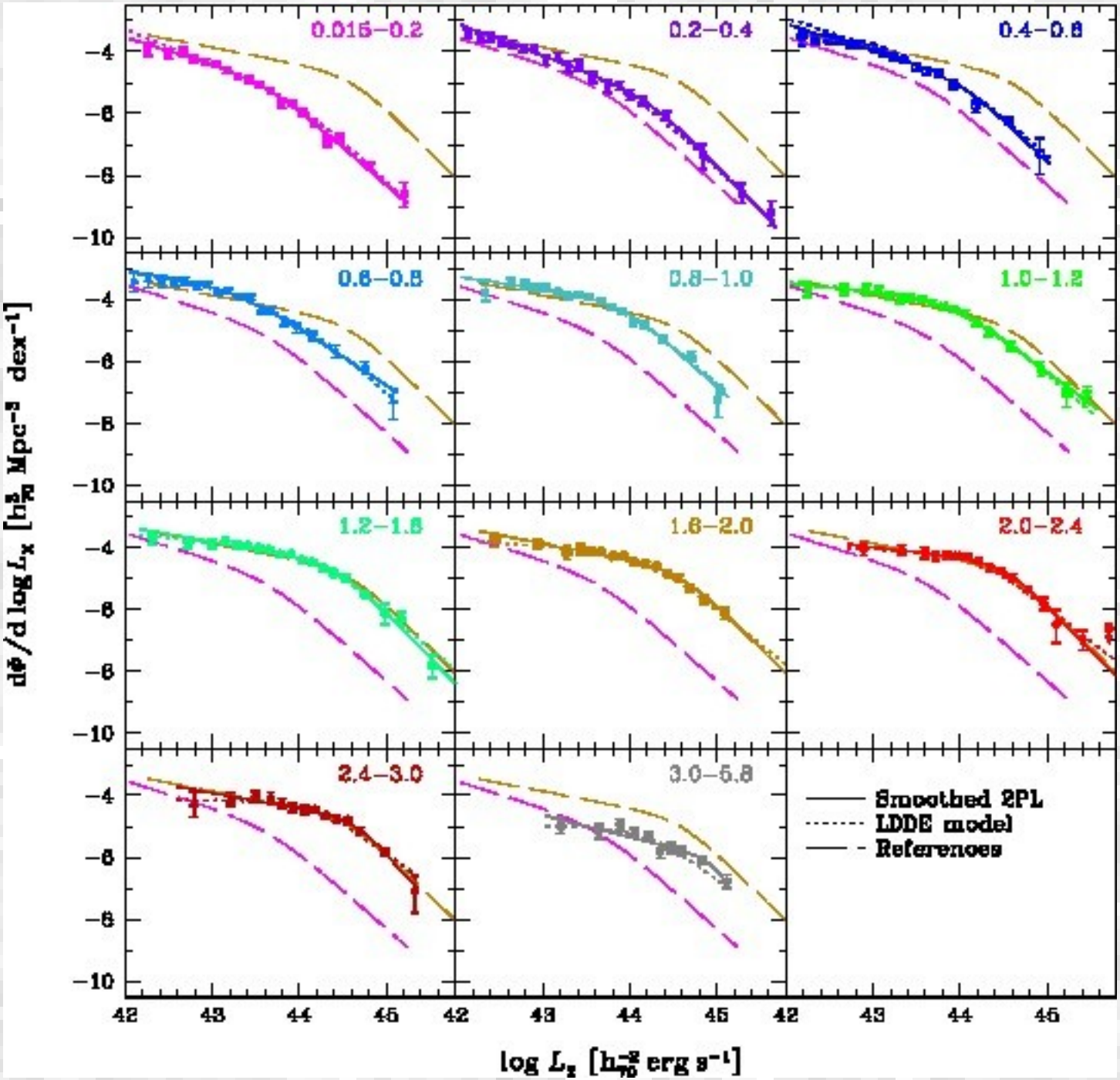

TM&COSMOS Team+2014

Key Features

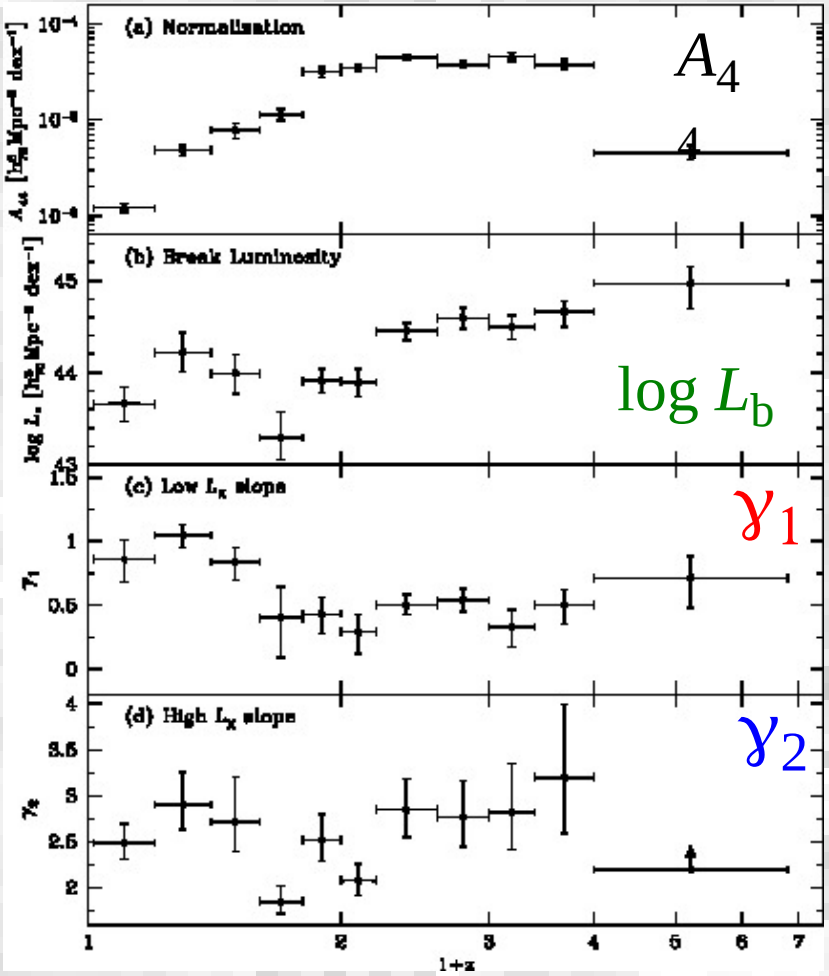

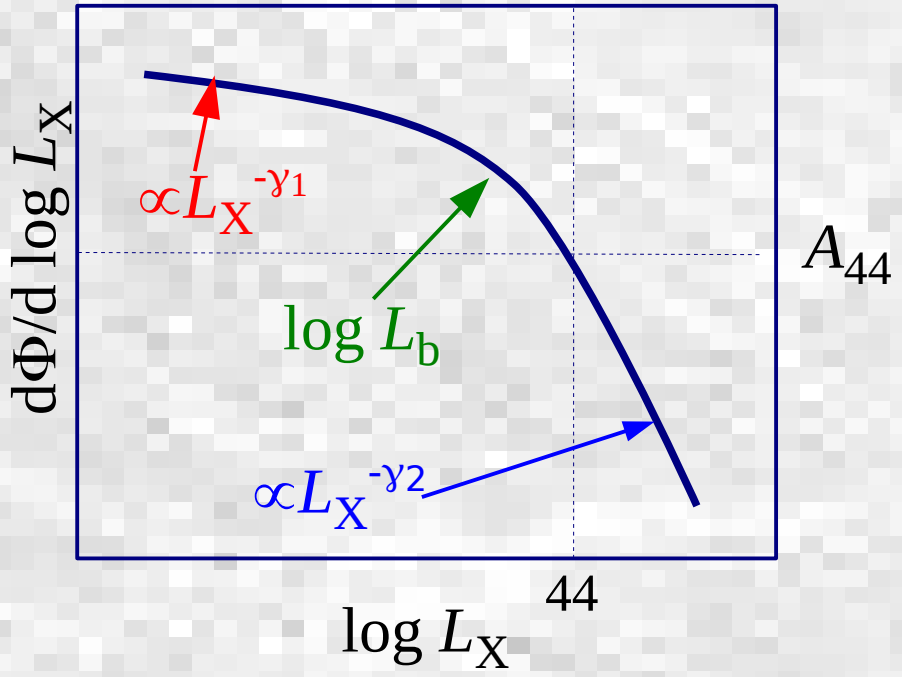

- In each redshift shell, the XLF is well represented by a smoothed two-power-law
- Normalization at log LX grows rapidly to z~1, stays flat, and drops at z>3.

- The high luminosity slope stays consisteny with γ_2~2.7 (with only a few exceptions, where high L end is not well constrained.)
- The low luminosity slope γ_1~1 at z<0.6, suddenly flattened to $\gamma_{\square}$~0.5 at z>0.6.

Cosmological Evolution of Number Density/Volume Emissivity

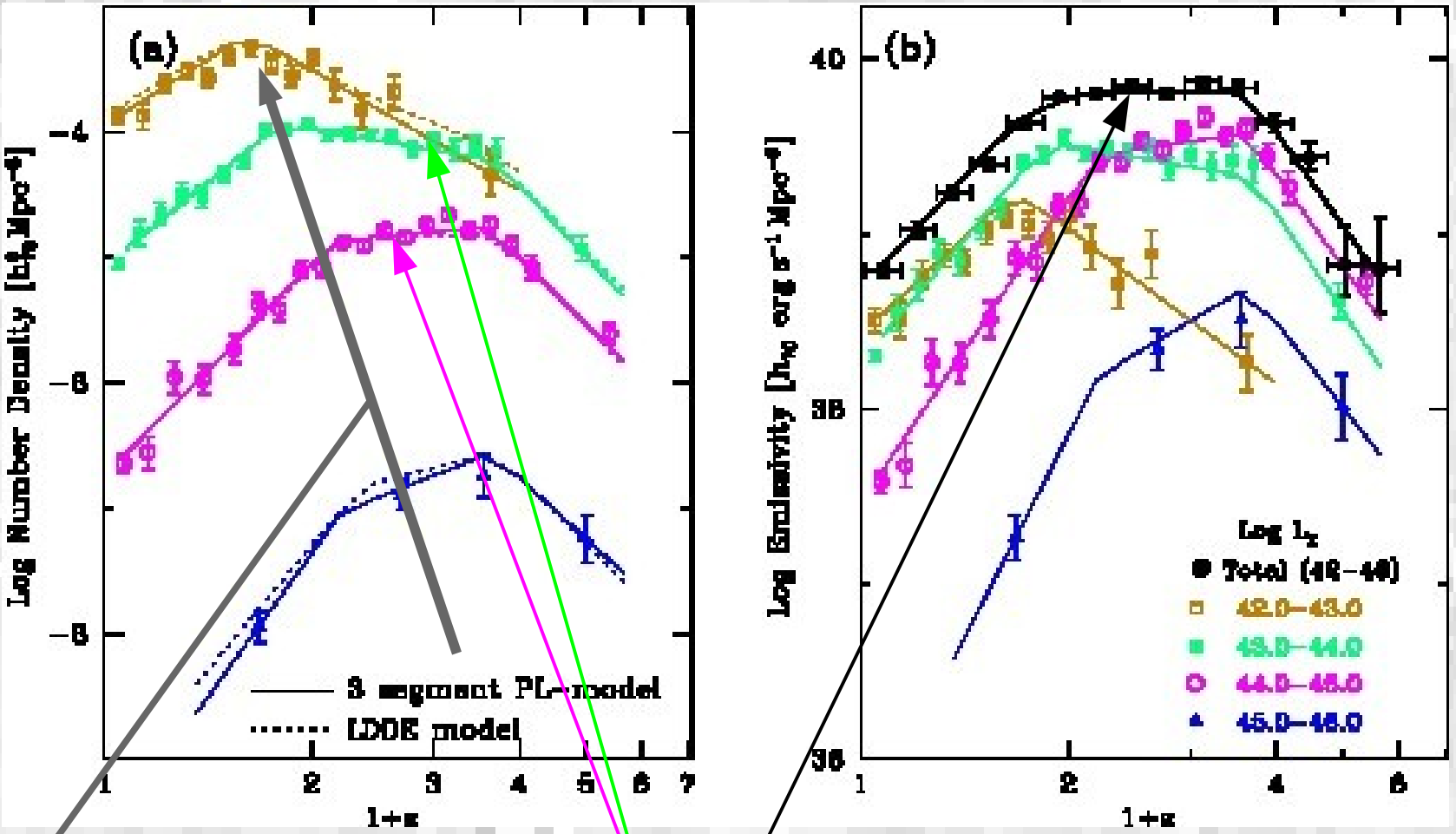

AGN downsizing

Flat top evolution

TM&COSMOS Team+'14

Comparison with other recent works

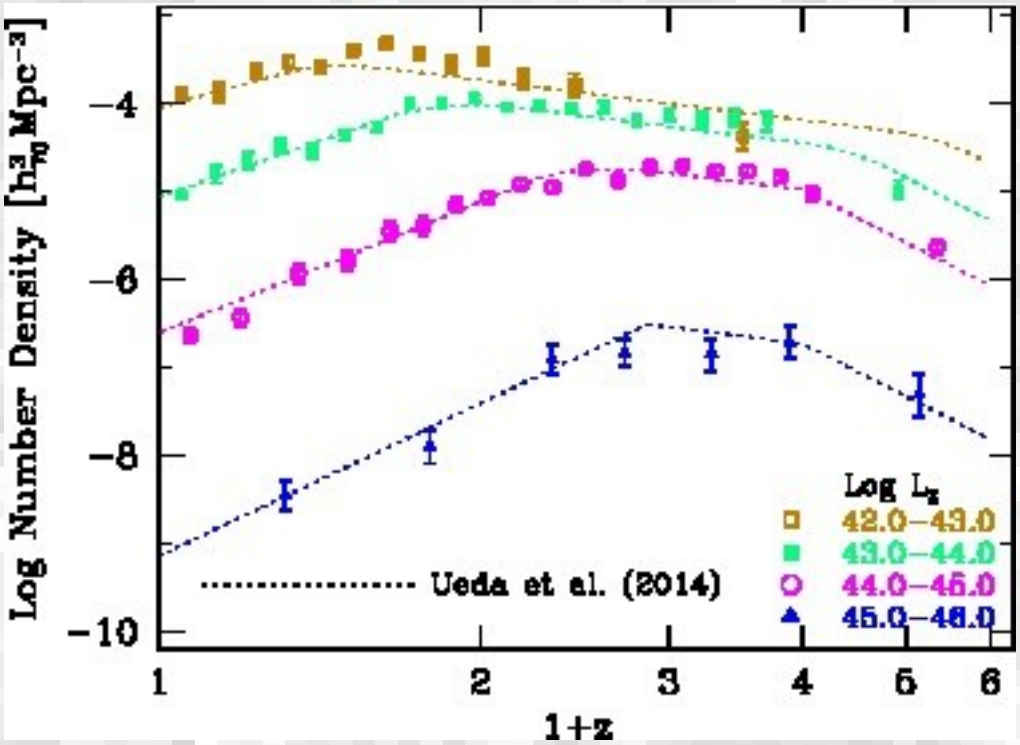

Miyaji et al. 2015 (data points) vs
Ueda et al. 2014 model comparison

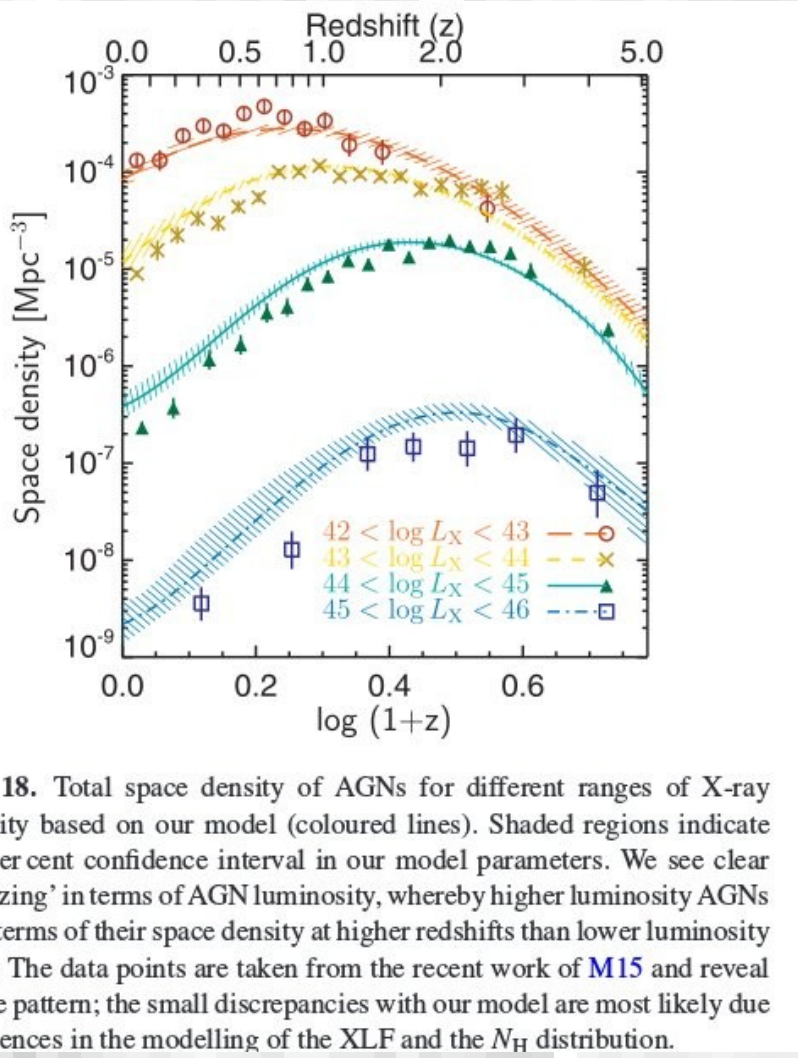

Figure 18. Total space density of AGNs for different ranges of X-ray luminosity based on our model (coloured lines). Shaded regions indicate the 99 per cent confidence interval in our model parameters. We see clear 'downsizing' in terms of AGN luminosity, whereby higher luminosity AGNs peak in terms of their space density at higher redshifts than lower luminosity sources. The data points are taken from the recent work of M15 and reveal the same pattern; the small discrepancies with our model are most likely due to differences in the modelling of the XLF and the N_H distribution.

Aird et al. 2015

Data points from TM+'15 compared with their best-fit analytical expressions.

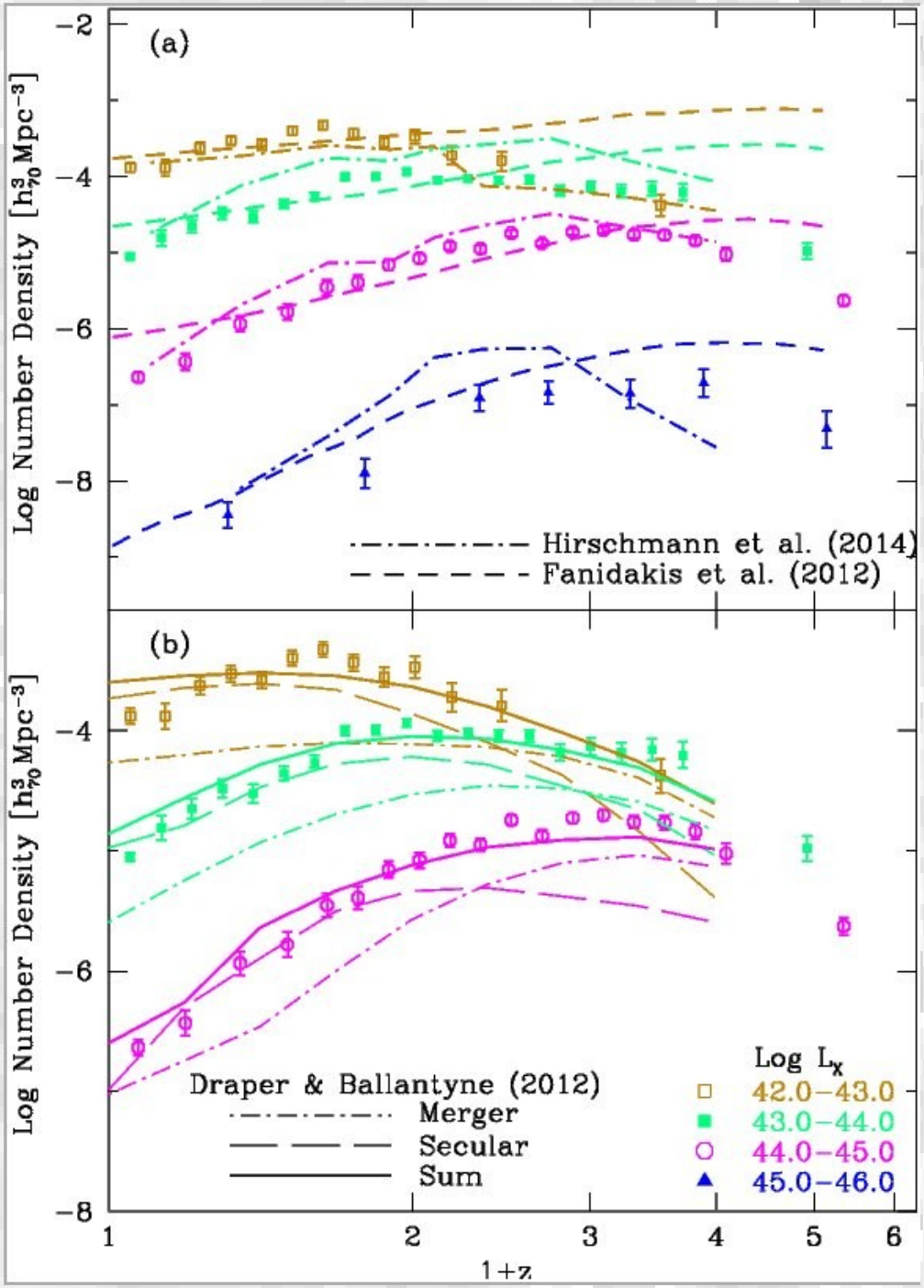

Comparisons with models

- Semi-analytical/simulation models:
  - Fanidakis+2012 (starburst mode incl. merger and disk instability+Hot halo gas)
  - Hirschmann+2014 (overpredicts number densities of high redshift/low luminosity AGNs.
- Draper & Ballantyne (2012) (merger+secular) reproduces the behavior of the number density curves well.

Secular

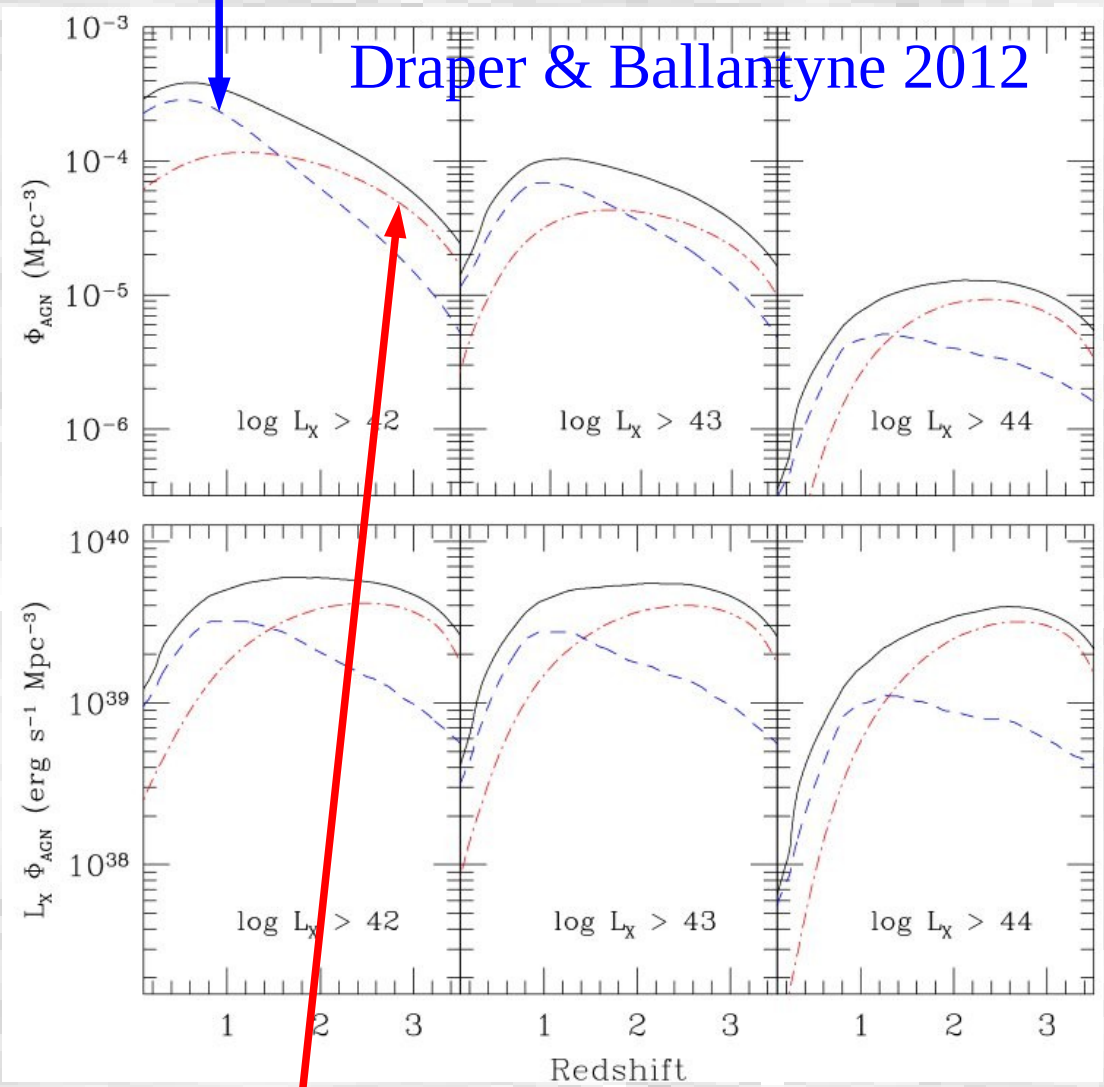

Merger

- .Draper & Ballantyne (2012) (merger+secular) reproduces the flat-top structure of the number density curves well.
- Not based on their own simulations. Based on analytical approximations from lietrature of:
  - Stellar Mass function (Perez-Glozales+'08)
  - Fraction of gas rich galaxies (Dahlen+'07; Treister+'10)
  - Merger rate (Hopkins+10)
- Three adjustable parameters of AGN light curve (some freedom).
- Cannot explain the number density evolution with only one of these componets. Both are needed.

Summary of XLF study

- Hard X-ray Luminosity function of (Compton-thin) AGNs have been constructed using a combination of ~3200 AGNs collected from various surveys.
- Addition of COSMOS survey enabled us to trace detailed behavior of XLFs in the intermediate redshift-luminosity range.
- Observed almost constant high L_X end slope, while the low LX end slope flattenes suddenly at z>0.6.
- Semi-analytical models based on hot-halo+merger mode tend to over-produce the low luminosity high redshift AGNs.
- The Draper & Ballantyne+'12 model based on secular and merger reproduces the XLF behavior well, especially the flat-top structure of the luminosity-dependent number density curves.

Clustering of AGNs -Another Observational Clue-

- Simple characterization of how AGNs trace underlying mass: bias parameter

$$b_{\mathrm{AGN}}=(\delta\rho/\langle\rho\rangle)_{\mathrm{AGN}}/(\delta\rho/\langle\rho\rangle)_{\mathrm{mass}}$$

(contrast enhancement factor)

- Large bias $b>1$, when a tracer samples high tips of underlying mass density (Kaiser '84).
- The bias parameter of how AGNs distribute in the universe is an indicator of the mass of Dark Matter Halos in which they reside (M_{DMH}).
- This is measured through two-point correlation functions [2PCF], either AGN auto-correlation functions or cross-correlations through galaxies.

Clustering of AGNs -Another Observational Clue-

- Simple characterization of how AGNs trace underlying mass: bias parameter

$$b_{\mathrm{AGN}}=(\delta\rho/\langle\rho\rangle)_{\mathrm{AGN}}/(\delta\rho/\langle\rho\rangle)_{\mathrm{mass}}$$

(contrast enhancement factor)

- Large bias $b>1$, when a tracer samples high tips of underlying mass density (Kaiser '84).
- The l… the univ… atter Halo…
- This … functi… functions or cross-correlations through galaxies.

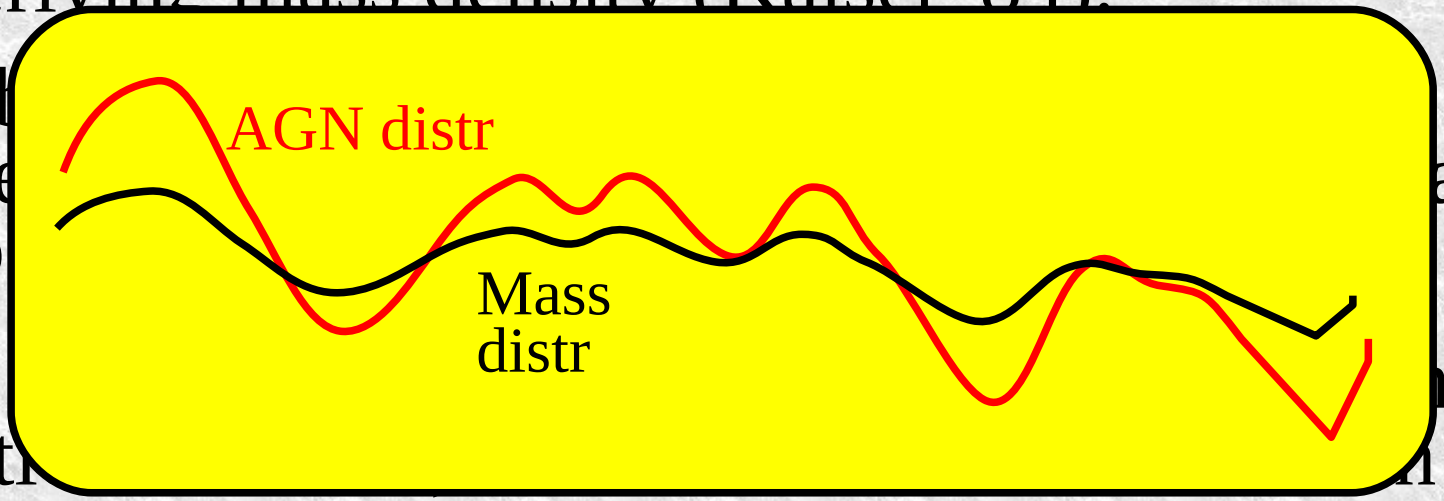

Clustering measurements→AGN bias

- The large-scale bias of dark matter halos depends on its mass.
- Here “Halo mass” means the mass of **largest Virialized structure** the objects belong to, and **NOT the sub-halo mass.**
- Measurements of bias of a sample of AGNs is an indicator of the “typical” mass of the DMHs that the sample is associated.

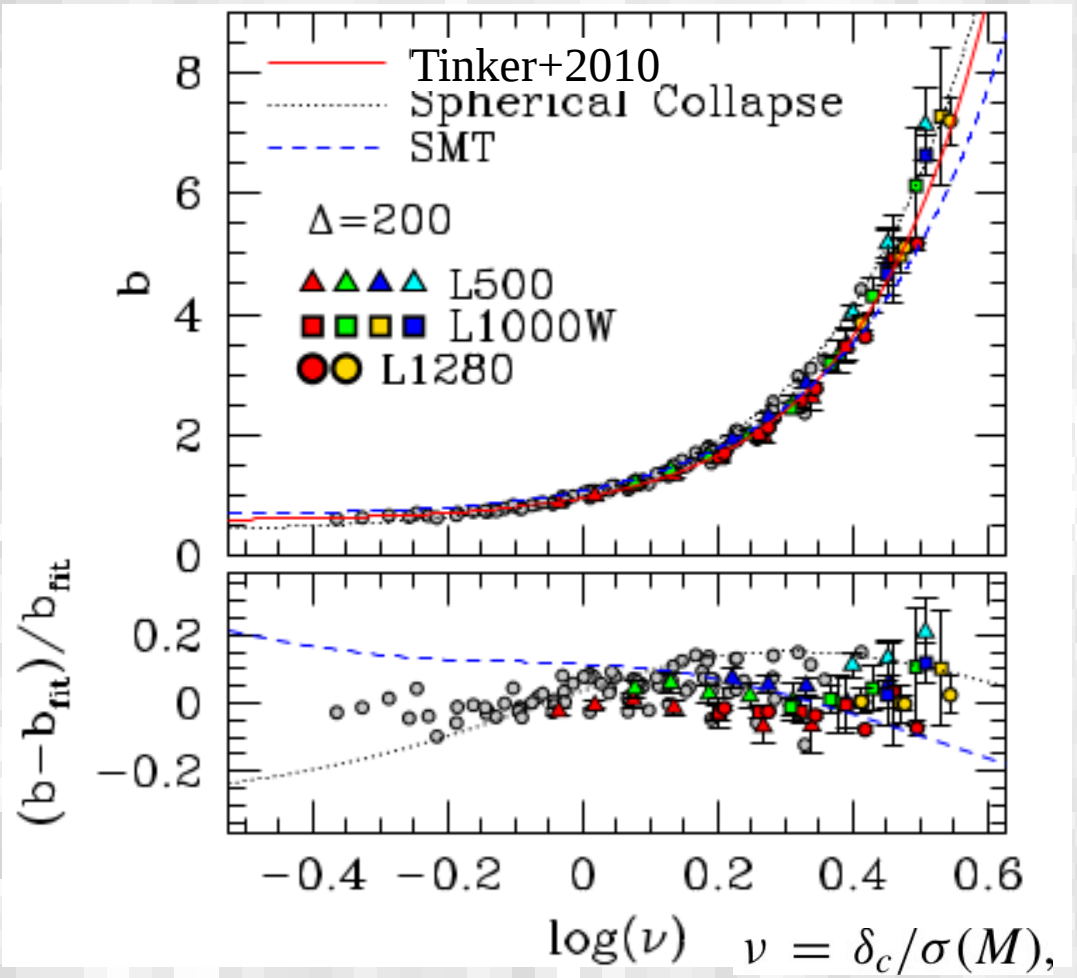

$$b_h(\nu) = 1 + \frac{1}{\sqrt{a}\delta_c}\left[\sqrt{a}(a\nu^2) + \sqrt{a}b(a\nu^2)^{1-c} - \frac{(a\nu^2)^c}{(a\nu^2)^c + b(1-c)(1-c/2)}\right]$$

This relation is only valid in the linear regime (r>~1-2 h^{-1} Mpc)

Cross-Correlation between SDSS Galaxies and ROSAT All-Sky Survey AGNs

Krumpe, Miyaji, Coil et al. 2009; Miyaji, Krumpe, Coil, Aceves 2011

- Galaxy Sample
  - SDSS LRG Volume Limited Sample
  - Defined by Eisenstein et al. (2001), redrawn by us for DR4+
  - M_B<-21.2, 0.16<z<0.36
  - 45899 LRGs Galaxies
- **X-ray AGN sample:**
  - ROSAT All-Sky Survey (RASS) sources matched with the SDSS broad-line AGNs (Anderson et al. 2003; 2007).
    - 1552 AGNs in 0.16<z<0.36
  - Excluded Narrow-line AGNs.
  - Flux limited sample.

Our early base sample.

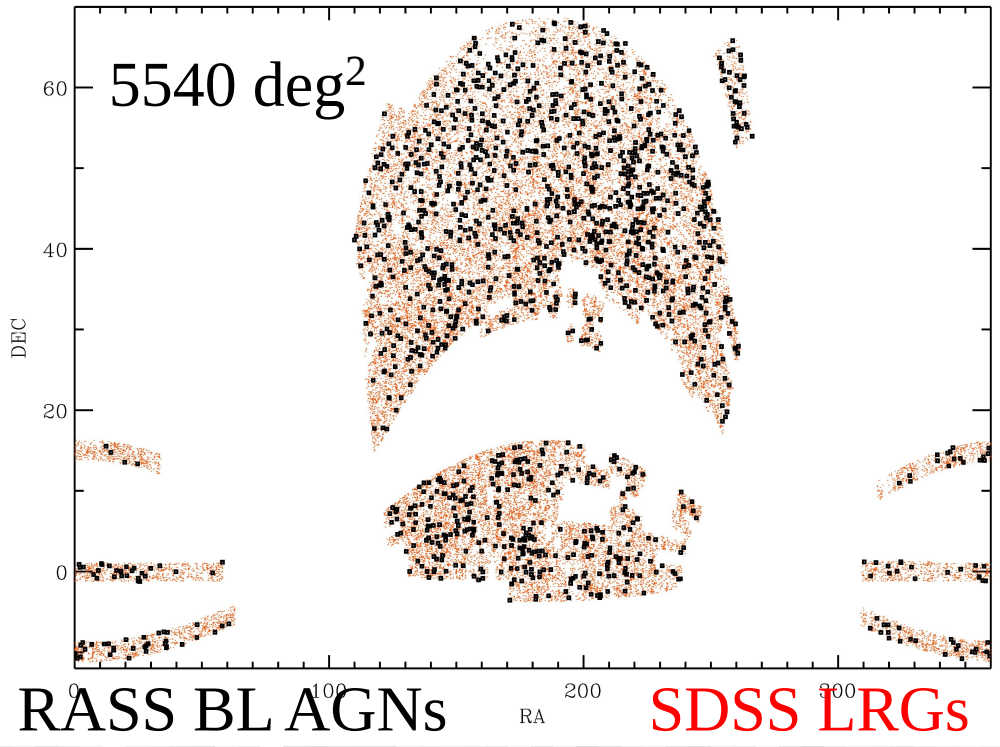

Modeling with Halo Occupation Distribution (HOD)

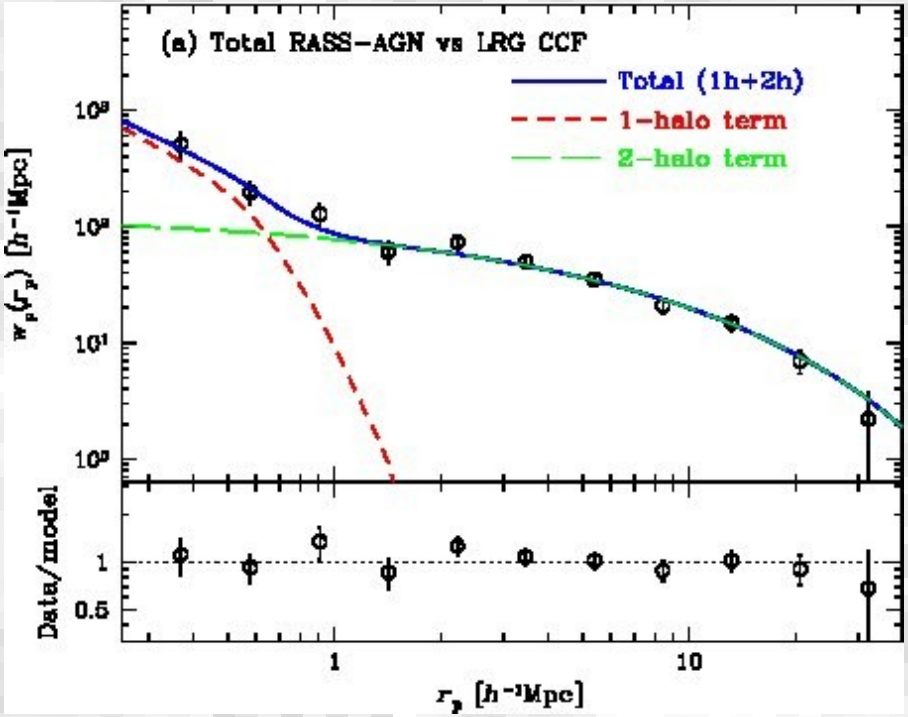

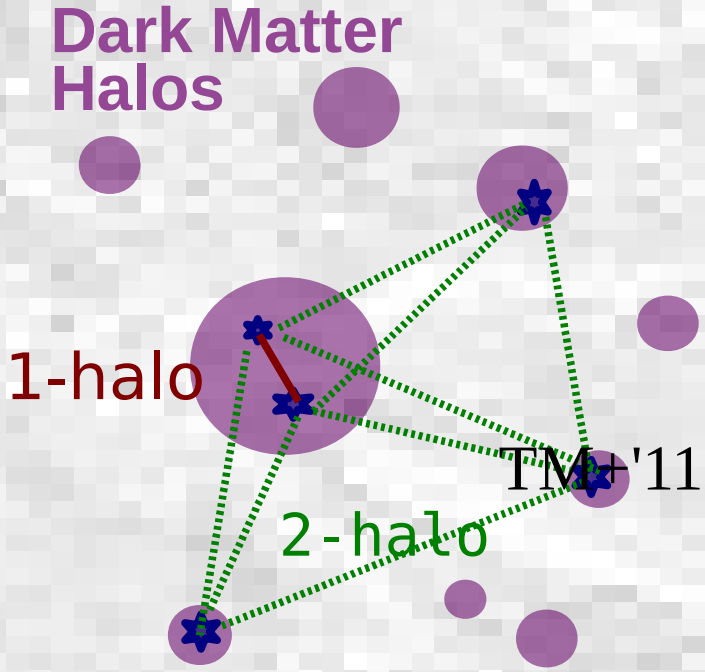

$$\xi(r) = [1 + \xi_{1h}(r)] + \xi_{2h}(r)$$

1-halo term 2-halo term

- Model the correlation function as the sum of the contributions from pairs:
  - within the same DMHs
  - from different DMHs.

Modeling with Halo Occupation Distribution (HOD)

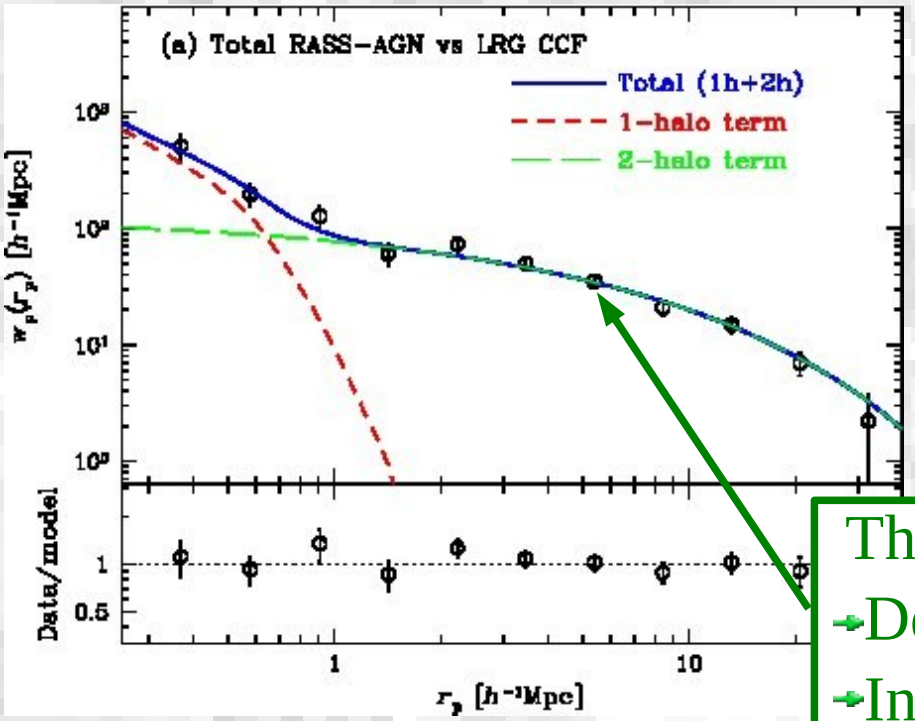

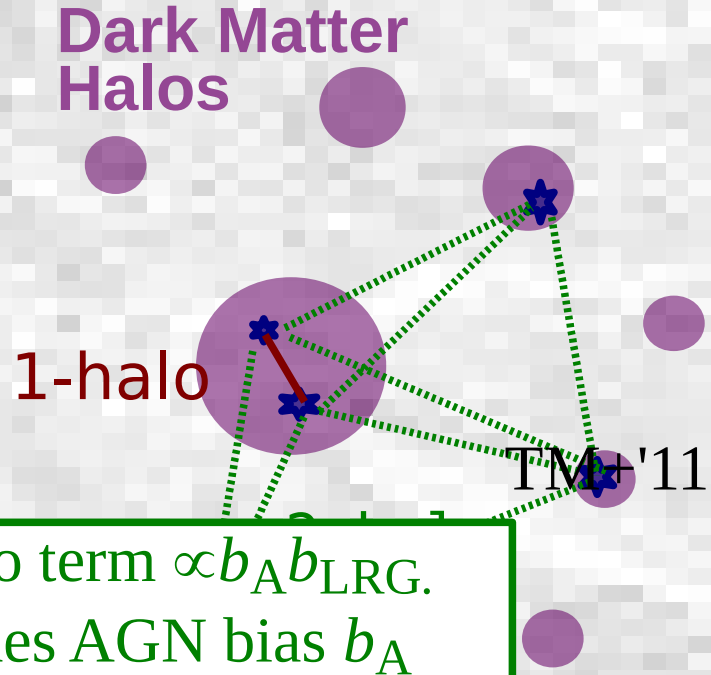

The 2-halo term $\propto b_A b_{LRG}$.

- Determines AGN bias b_A
- Indicates the mean DMH mass with AGNs.

…on function as the sum of the contributions from pairs:

- within the same DMHs
- from different DMHs.

$$\xi(r) = [1 + \xi_{1h}(r)] + \xi_{2h}(r)$$

1-halo term 2-halo term

bias (M_{DMH})

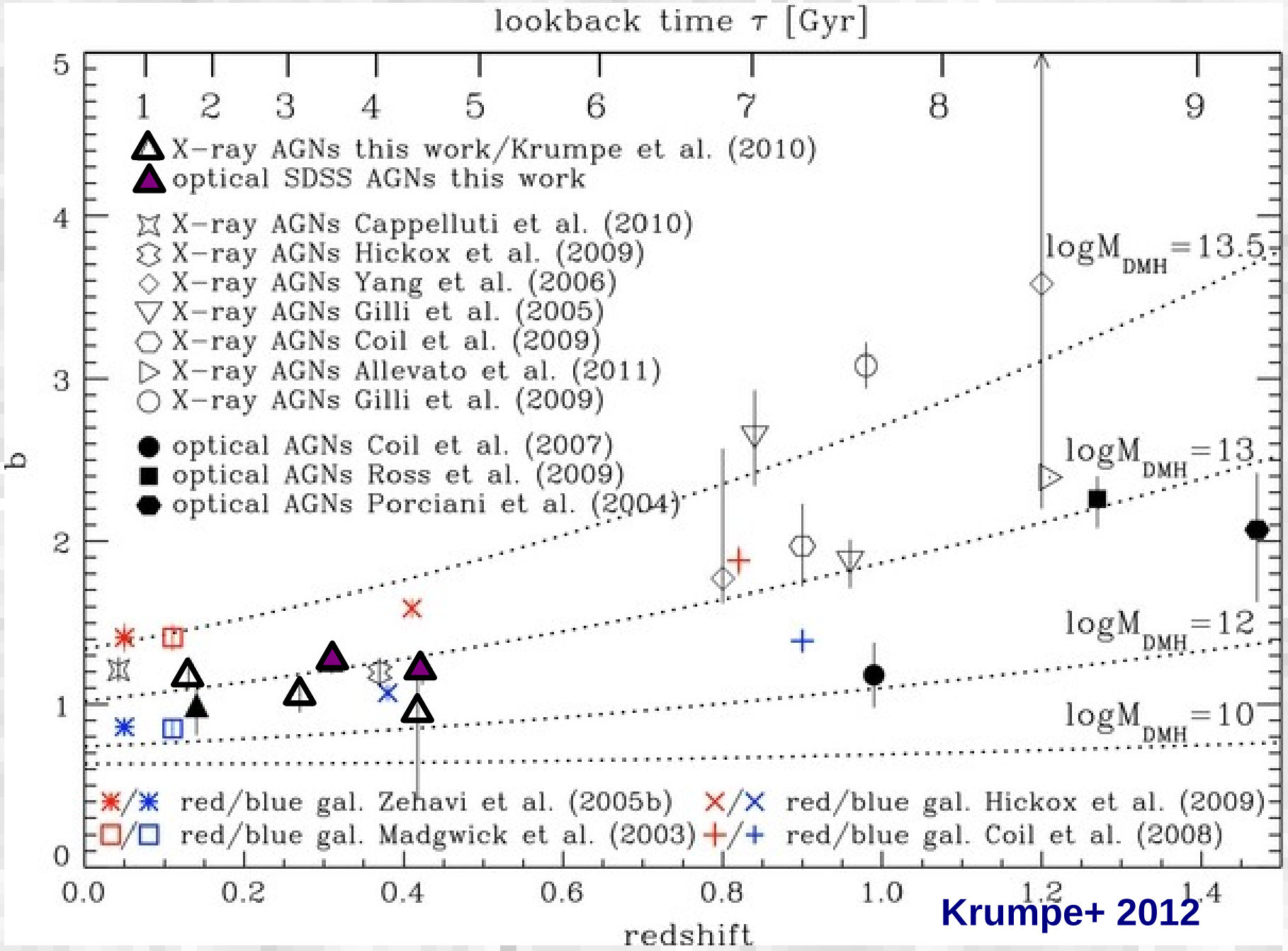

Krumpe+ 2012

Bias scales with M_{BH} but not with L/L_{edd}

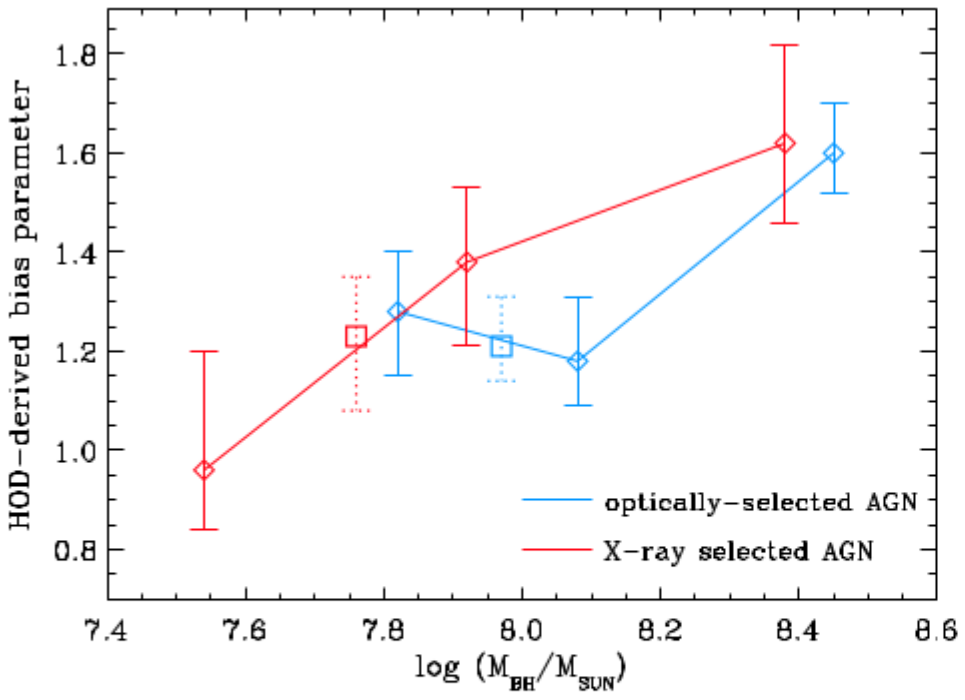

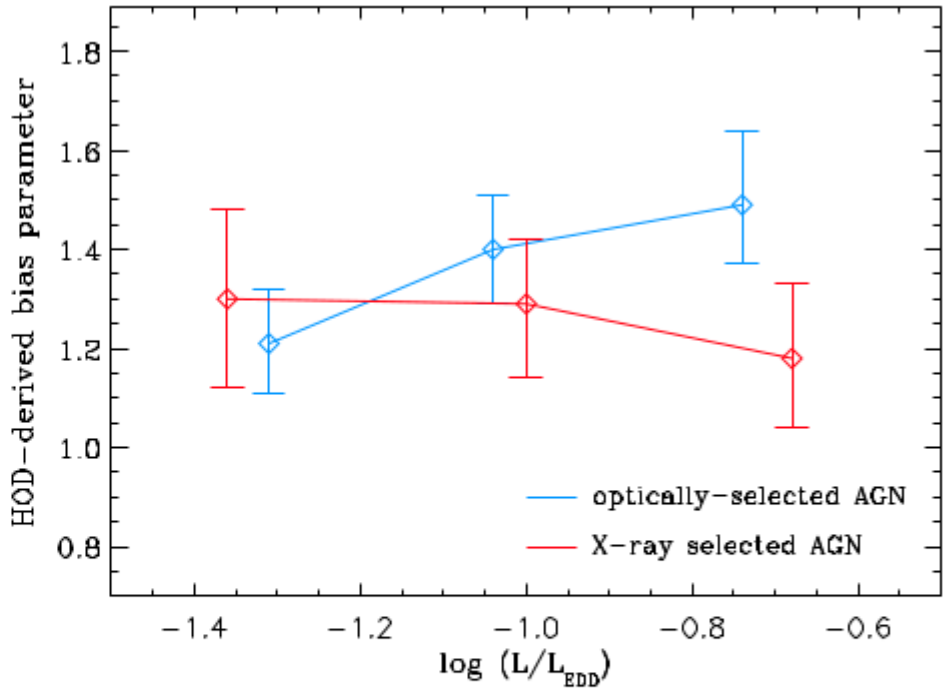

FIG. 10.— *Left:* HOD-derived bias parameter as a function of SMBH mass for the optically-selected SDSS (blue) and the X-ray selected RASS/SDSS AGN sample (red). The data points shown as diamonds represent a split of the total sample in $M_{\rm BH}$ into 30% (high), 40% (medium), and 30% (low) $M_{\rm BH}$. The boxes (with dotted error bars) indicate the combined medium and low $M_{\rm BH}$ subsamples. All data points are plotted at their median $M_{\rm BH}$ of the corresponding subsample.
Right: Similar to the left panel. Now showing the HOD-derived bias parameter as a function of Eddington ratio.

Krumpe, TM et al. 2015 ApJ submitted

Comparison with a SAM model (0.16<z<0.36)

(by N. Fanidakis)

DMH mass

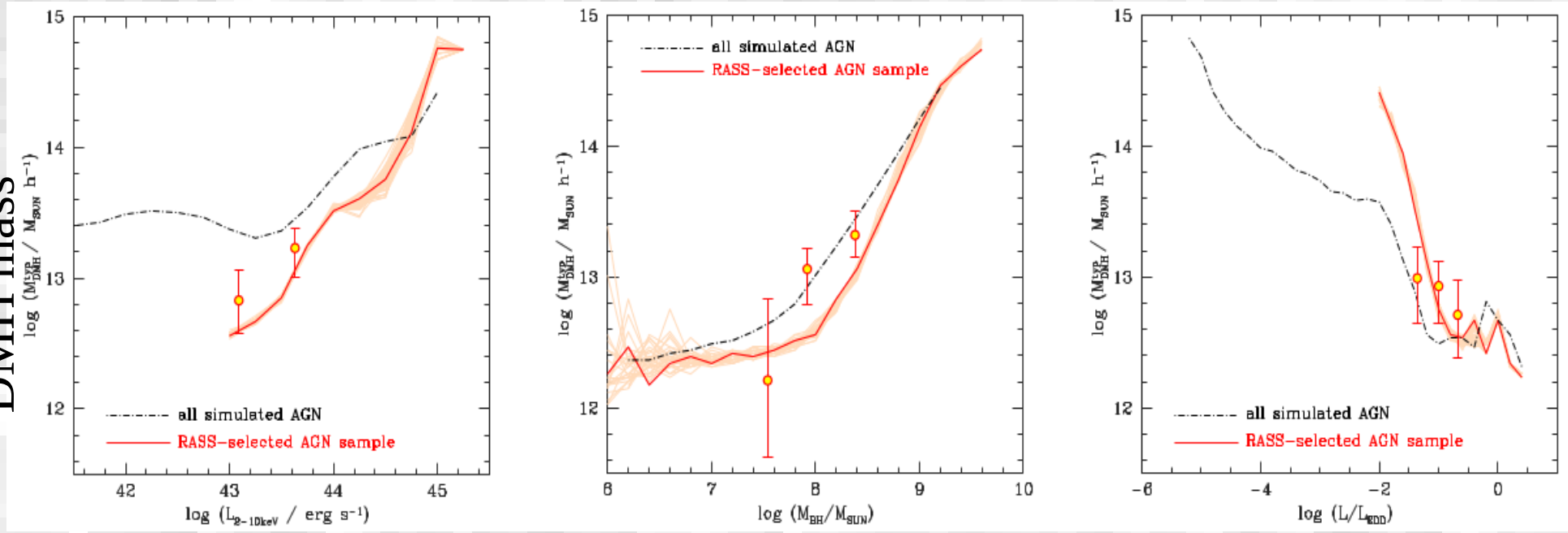

log L_X log M_{BH}/M_{sol} log L_{bol}/L_{Edd}

Red Data Points: Observation
Orange Lines: Simulation with RASS selection
Black Lines: Simulation, all AGNs

Krumpe, TM et al. (incl. N. Fanidakis) 2015 ApJ submitted

Xray selected AGNs in the COSMOS Field

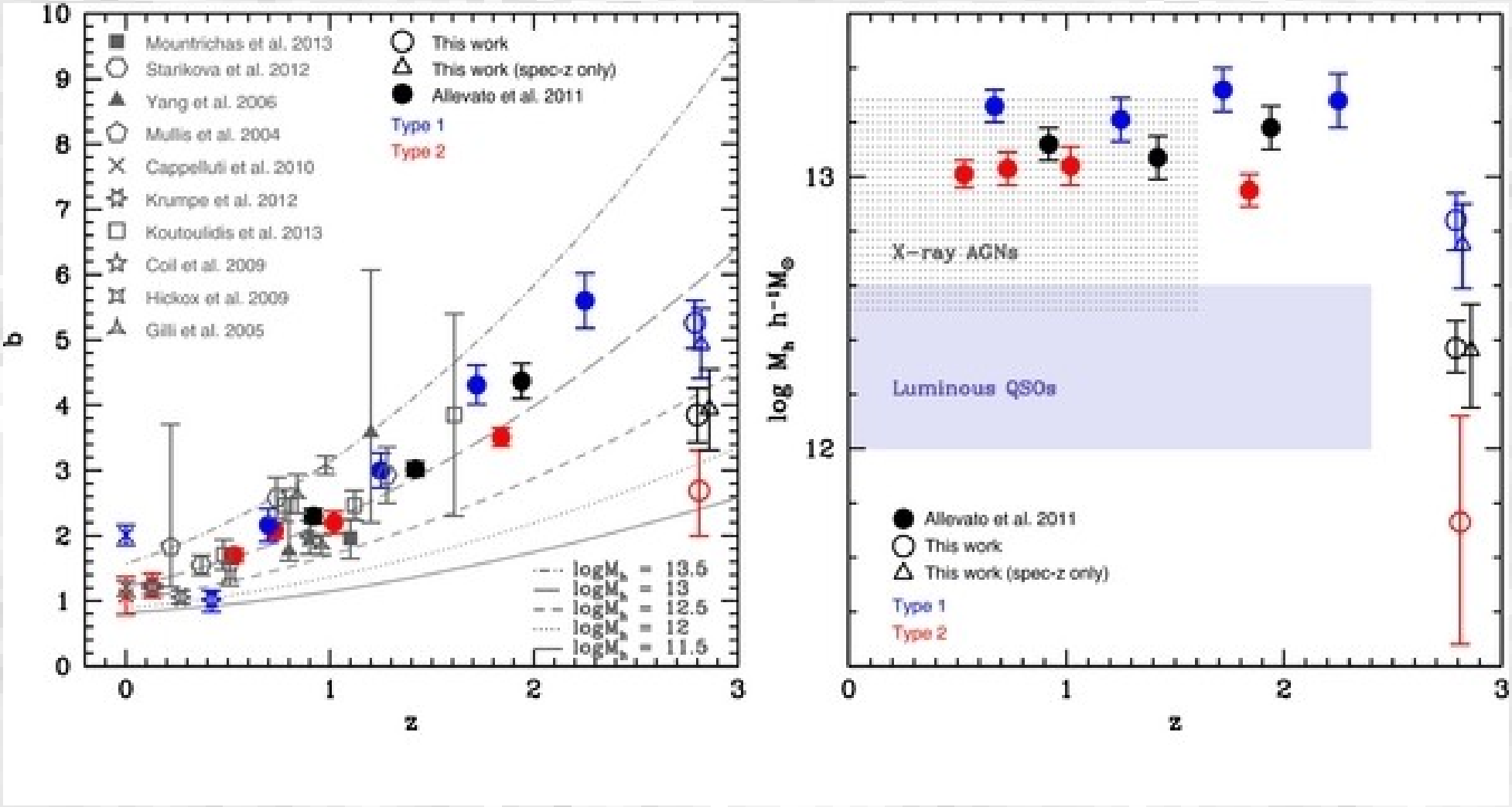

Allevato et al. 2014

z~3 Bias

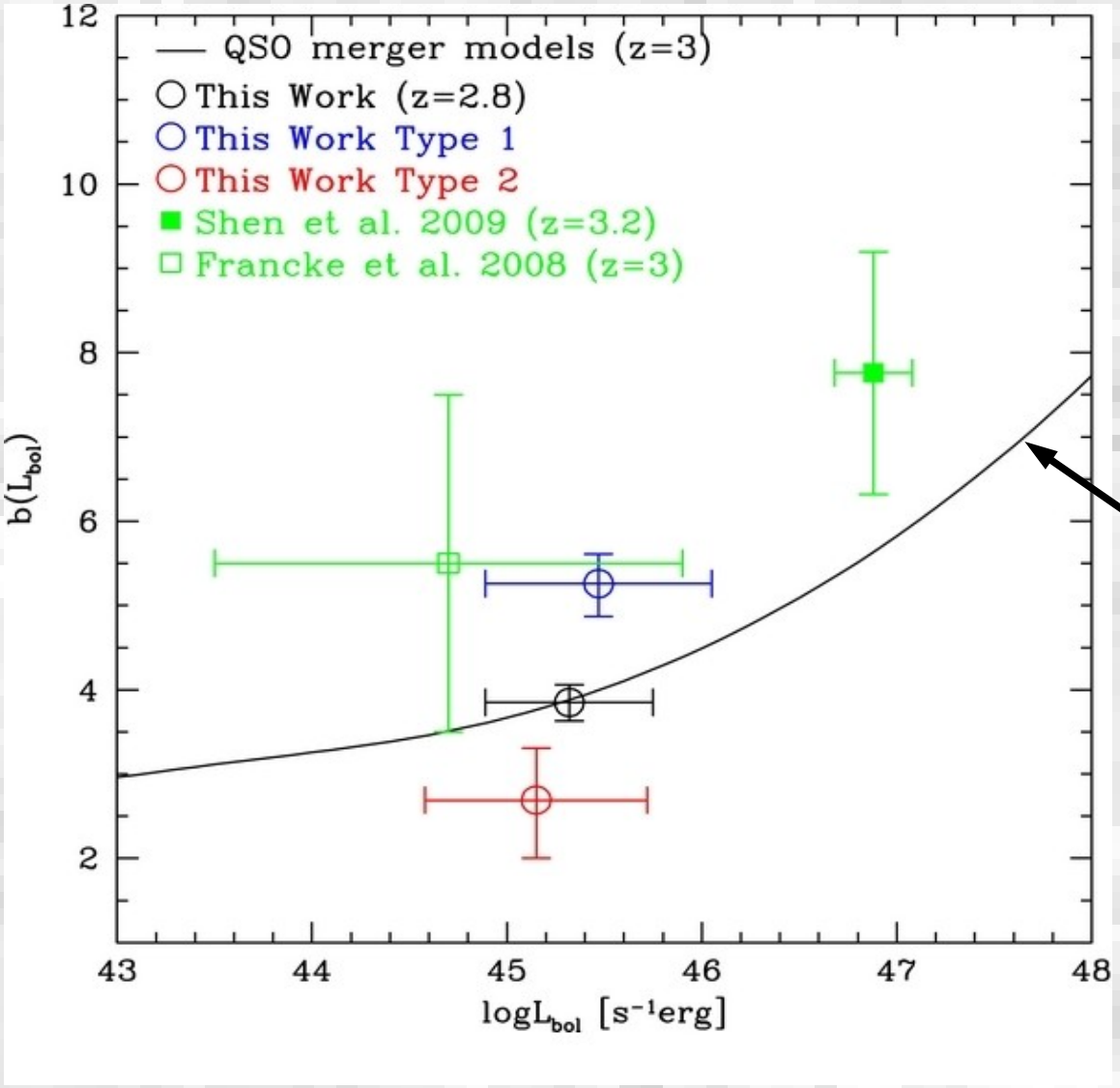

Shen et al. (2009) Halo merger model. (Does not include sub-halo mergers)

Allevato et al. 2014

Luminosity dependence of host halo mass in cosmological simulations (Hot halo mode+starburst mode)

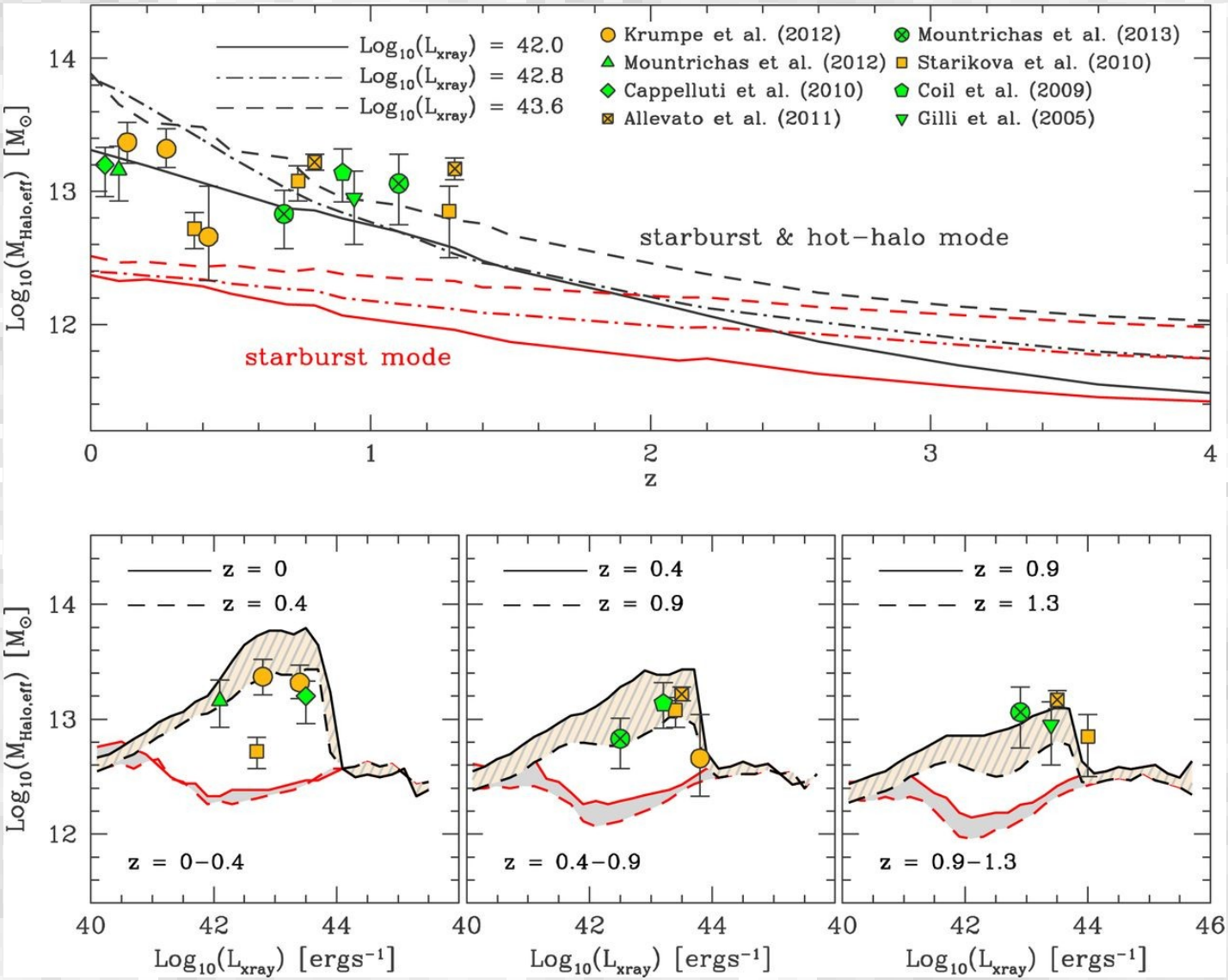

Fanidakis+'13

Key Results of AGN bias (Typical DMH mass)

- X-ray selected AGNs with moderate luminosities (log L_X~43-45 [erg s^{-1}]) at z~0.3 (Krumpe+) and z~1 (Allevato+'11) are hosted typically by log M_{DMH}~13-13.5 [M_{sol}] DMHs **(More strongly clustered than the merger scenario by Shen et al. 2009)**.
- Weak positive X-ray luminosity dependence of M_{DMH} within the range of log L_X~43-45 [erg s^{-1}] at z~0.3. This is caused by the black hole mass and not L/L_{edd}.
- Optical luminous QSOs at z>~1 are associated with log M_{DMH}~12-12.5 [M_{sol}], typically lower than those of modest luminosity X-ray selected AGNs and consistent with a merger scenario **(Reverse luminosity dependece).**
- X-ray selected AGNs at z~3 are associated with log M_{DMH}~12-12.5 [M_{sol}] DMHs. **(Consistent with the merger scenario)**

1-halo term constraints

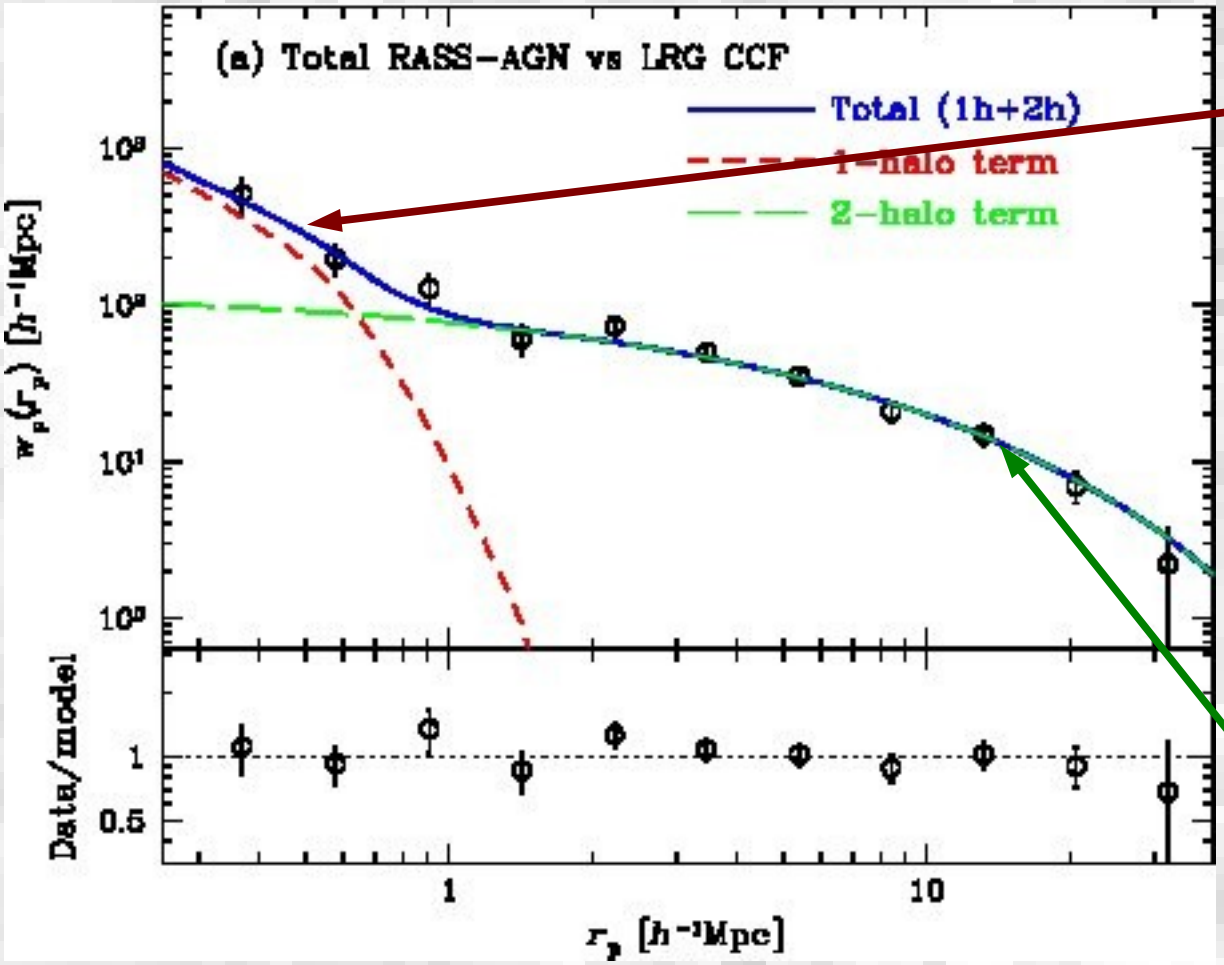

The 1-halo term is from AGN-LRG pairs in the **same DMH**.

- LRGs are in M_h>~$10^{13.5}$ $M_\odot$ halos.
- The 1-halo term measures AGNs in M_h>~$10^{13.5}$ $M_\odot$ DMHs.

The 2-halo term $\propto b_A b_{LRG}$.

- Determines AGN bias b_A
- Indicates the mean DMH mass with AGNs.

Miyaji et al. 2011

Constraints on HODs for AGNs

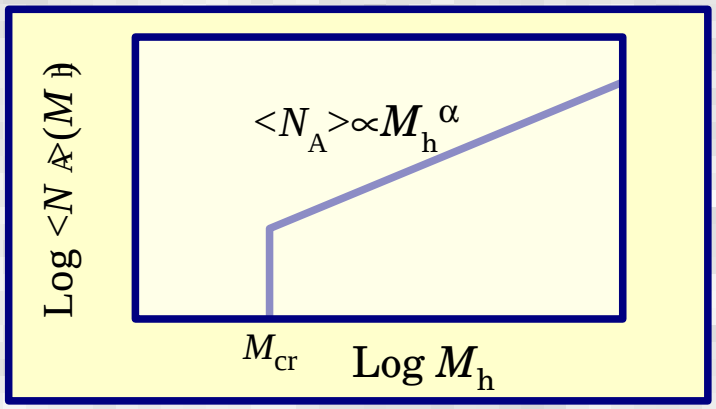

Simple HOD model for AGNs (Center + Satellites)

- Constraints roughly along $\langle M_h \rangle$~const.
  - Constraint from the 2-halo term (b_X)
- α<0.4 ($\Delta\chi^2$<2.3 limit)
  - Constraint from the 1-halo term

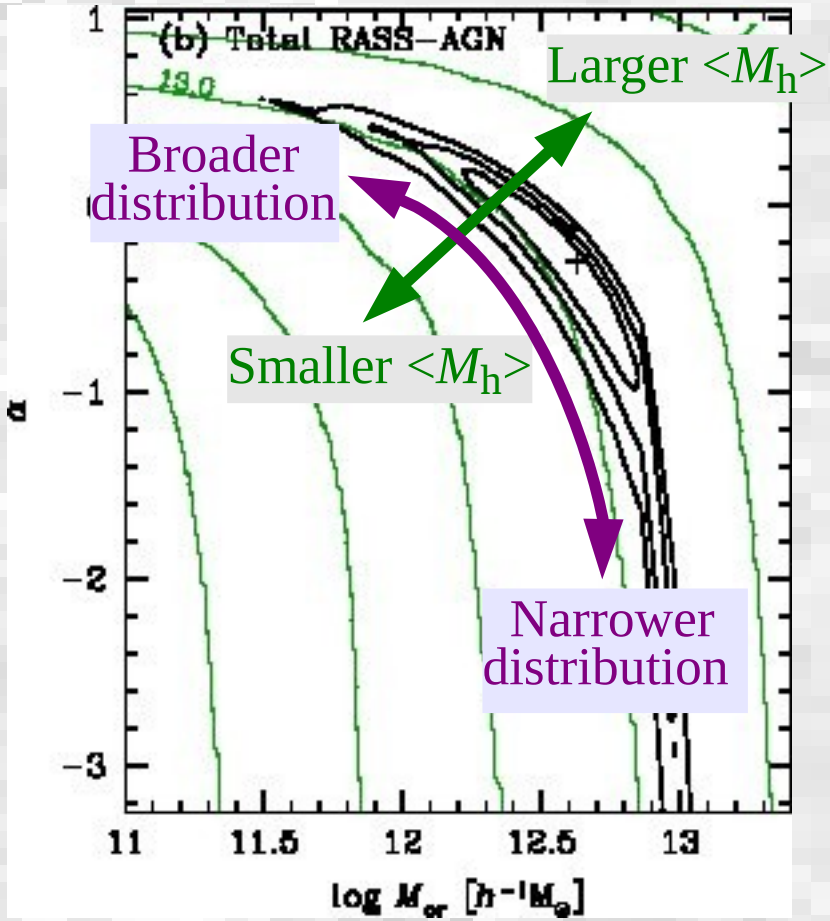

- Confidence contours (black, $\Delta\chi^2$=1;2.3;4.6)
- Mean DMH mass (green contours).

Model with separate central+satellite AGNs

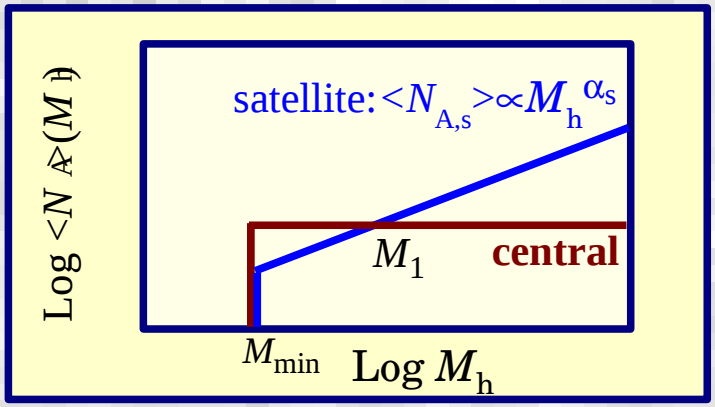

Model B:
A model with galaxy-like central+satellite components
α_s<0.9

cf. SDSS Galaxies
(e.g. Zehavi et al. 2005)
$M_1/M_{min} \approx 23$, $\alpha_s \approx 1.2$

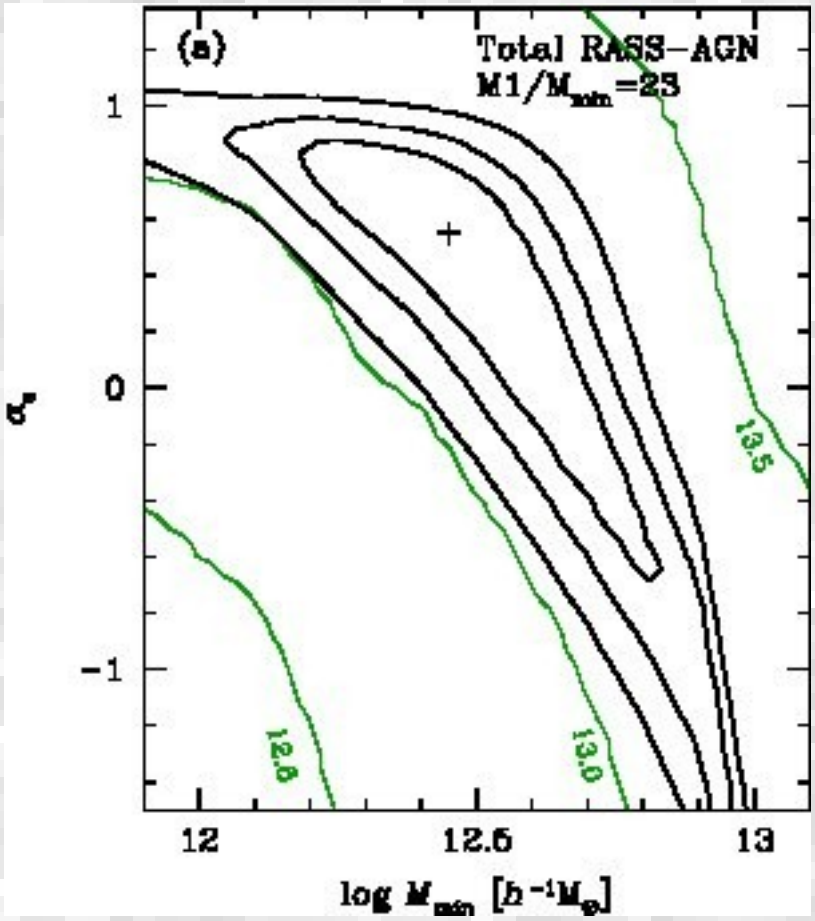

Trend Verified in direct counts in resolved X-ray groups in the COSMOS survey

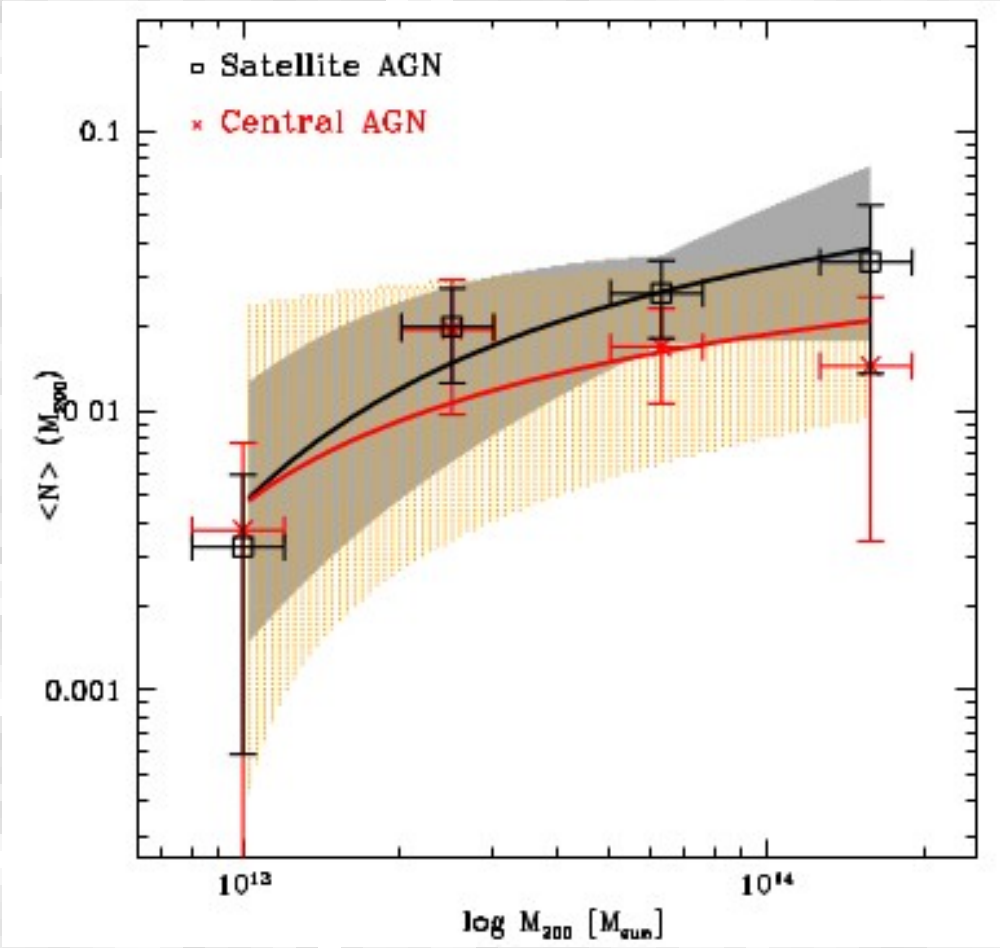

Allevato+12, direct count. Satellite HOD slope α_s<0.63

Implication of the HOD Analysis

- The limit on α_s<1 means that the number of (satellite) AGNs/Halo ***grows slower than M_h***.
  - The HOD of satellite **galaxies** show α~1, i.e., number/halo $\propto M_h$ (e.g. Zehavi et al. 2010).
  - AGN fraction (non-center) decreases with M_h.
  - X-ray AGN fraction is smaller in clusters ($M_h > 10^{14} M_{sol}$) than the field at low z. Higher at high z (z>~1.5), this trend reverses (Martini+13).

Possible Machanisms

- Under a scenario where AGNs are triggerd by sub-halo sub-halo mergers, merging cross-section low in high velocity encounters (Makino & Hut 1997).
  - Would AGN triggering by major merger/minor merger of **sub-halos** inside larger host halos explain the HOD behavior? -> **Check in cosmological simulations (L. Altamirano's thesis work with H. Aceves+TM).**
- Ram pressure stripping of cold gas in Intracluster/intragroup medium.

Checking sub-halo merger scenario with N-body Simulations

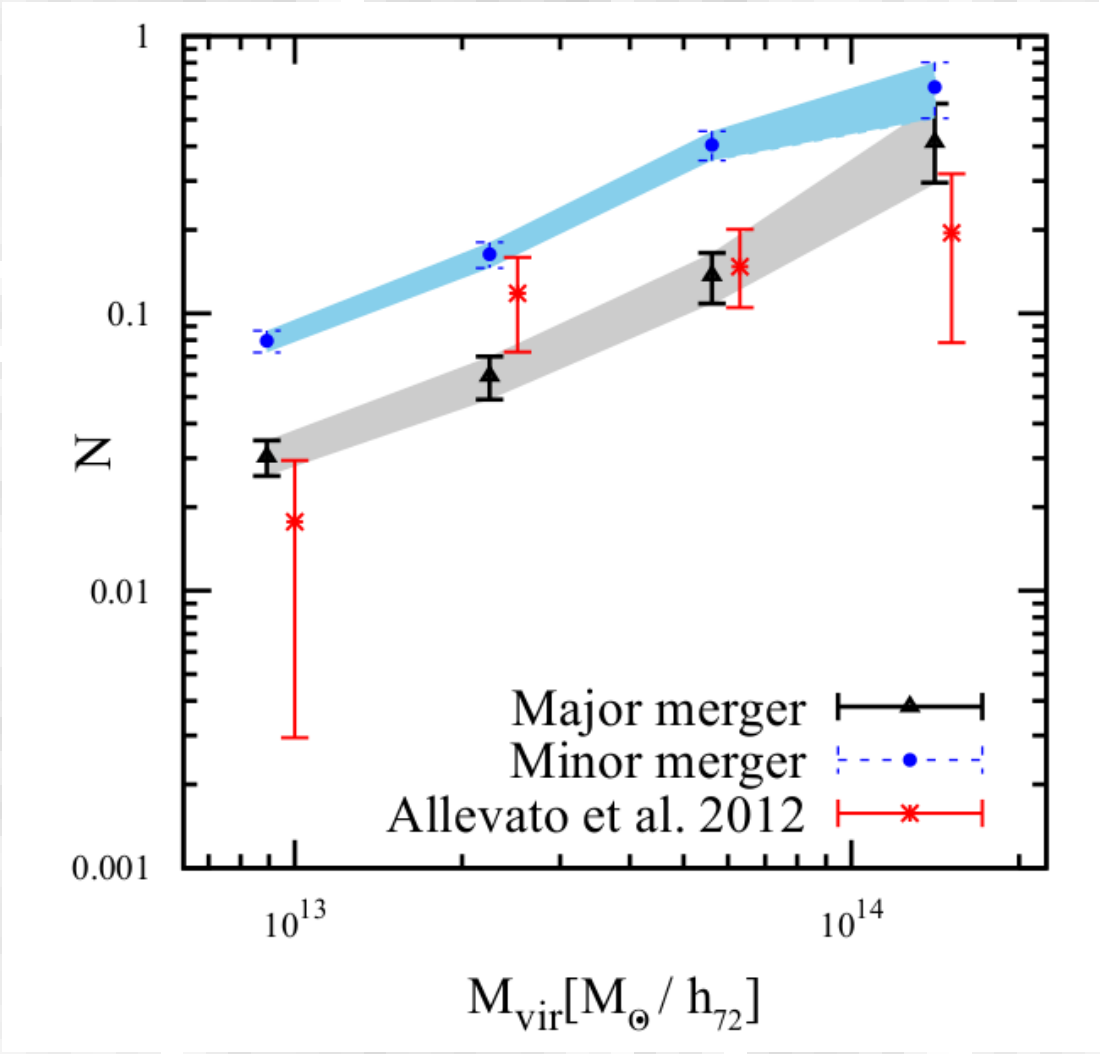

TABLE 1

NUMBER DENSITIES AND HOD SLOPES

Mechanism	n_{agn}	α_s
Major	2.28×10^{-5}	0.20 ± 0.18
Minor	5.96×10^{-5}	0.10 ± 0.09
Observed[1]	4.2×10^{-5}	$0.22^{+0.41}_{-0.29}$

[1] Allevato et al. (2012)

Altamirano, Miyaji, Aceves et al. (2015) RmxAA, submitted

Summary on AGN clustering

- X-ray selected AGNs with log L_X~44 at z<2 are typically associated with~10^{13}-$10^{13.5}$ $M_\odot$ DMHs, i.e. groups of galaxies. At z~3, the host DMH masses are ~10^{12}-$10^{12.5}$ $M_\odot$.
- Much more luminous population of optical QSOs are associated with host DMH mass of typically ~10^{12}-$10^{12.5}$ $M_\odot$ (Negative dependence), and can be explained by a merger scenario.
- A weak positive X-ray luminosity dependence of $M_{DMH}$is observed at z~0.3. This is driven by the black hole mass rather than the Eddington rato.
- The luminosity, M_{BH} and L/L_{edd} dependences are consistent with a semi-analytical model with hot-halo+starburst modes.
- HOD analysis gives distribution of AGNs among DMHs in various mass. We find that AGN fraction among satellite galaxies decrease with Halo mass. This has been verified by direct X-ray AGN counts in X-ray resolved groups in the COSMOS field.